Sensorless Control of Non-salient Permanent Magnet Synchronous Motor Drives using Rotor Position Tracking PI Controller

Jong-Kun Lee* and Jul-Ki Seok †

Abstract – This paper presents a new velocity estimation strategy for a non-salient permanent magnet synchronous motor drive without high frequency signal injection or special PWM pattern. This approach is based on the d-axis current regulator output voltage of the drive system, which contains the rotor position error information. The rotor velocity can be estimated through a rotor position tracking PI controller that controls the position error at zero. For zero and low speed operation, the PI gain of the rotor position tracking controller has a variable structure according to the estimated rotor velocity. Then, at zero speed, the rotor position and velocity have sluggish dynamics because the varying gains are very low in this region. In order to boost the bandwidth of the PI controller during zero speed, the loop recovery technique is applied to the control system. The PI tuning formulas are also derived by analyzing this control system by frequency domain specifications such as phase margin and bandwidth assignment.

Keywords: Non-salient permanent magnet synchronous motor drive, d-axis current regulator output voltage, rotor position tracking controller.

1. Introduction

The Permanent Magnet Synchronous Motor (PMSM) is gradually replacing classic DC motors in many industrial applications. This has been made possible due to the attractive features of the PM motor such as its compactness, high efficiency, robustness, and high power density. However, in order to achieve accurate information pertaining to the rotor position, the PMSM drives require a position sensor. The first generation of sensorless control is based on rotor flux orientation by integration of back emf [1-3]. These approaches require motor electrical parameters and fail at low and zero speeds since the back emf information is excessively low.

Recently, simpler and more effective algorithms have been developed, such as the high frequency injection method and the constant frequency pattern method [4-5].

The high frequency injection method uses the impedance difference of the motor and can successfully obtain the position information even at low and zero speeds [4]. However, the high frequency excitation usually requires a signal processing technique and may cause undesirable side effects such as torque oscillation, harmonic losses, and acoustic noise. It also limits the speed range below one hundred Hz due to extraction of the injected signal.

In the constant frequency pattern method [5], the speed is estimated by processing the output voltages of the d-axis PI current regulator in high speed range and the current with a constant magnitude, while a pre-patterned frequency is injected from startup to low speed range. This scheme provides extremely accurate and robust speed information in the high speed range. However, it requires an extra transition algorithm and cannot perform vector control in the low speed region.

This paper presents an innovative velocity estimation strategy for a non-salient permanent magnet synchronous motor drive without high frequency signal injection or special PWM pattern. This approach is based on the d-axis current regulator output voltage of the drive system, which contains the information pertaining to the rotor position error. The rotor velocity can be estimated through a rotor position tracking PI controller that controls the position error at zero. For zero and low speed operation, the PI gain of the rotor position tracking controller has a variable structure according to the estimated rotor velocity. Then, at zero speed, the rotor position and velocity have sluggish dynamics because the varying gains are quite low in this region. In order to boost the bandwidth of the PI controller during zero speed, the loop recovery technique is applied to the control system. Analyzing this control system by the frequency domain specification such as phase margin and bandwidth assignment, the PI tuning formulas are also derived.

† Corresponding Author: Dept. of Electrical Engineering, Yeungnam University, Korea. (doljk@yu.ac.kr)
* Robot Institute, Daewoo Shipbuiding & Marine Engineering Company Ltd. Korea.
Received April 3, 2004 ; Accepted August 25, 2004

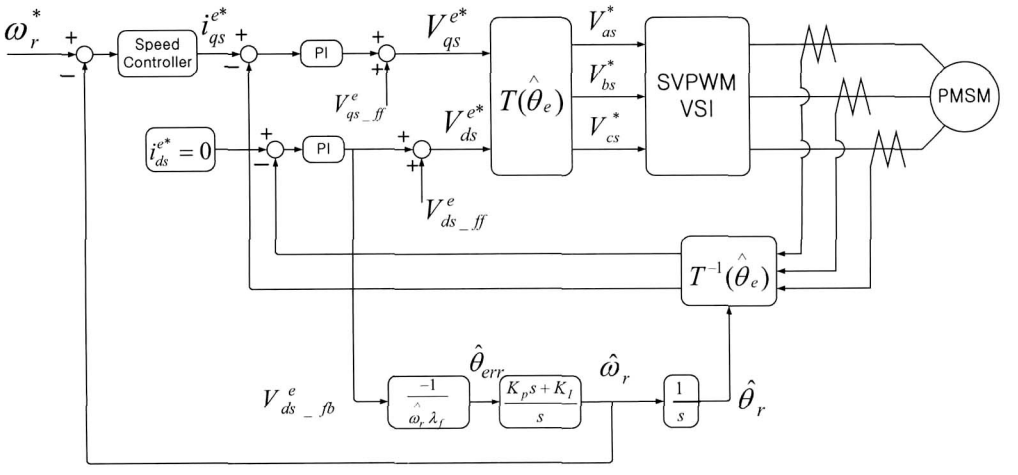

Fig.1 Block diagram for overall control structure of constant frequency pattern method

2. Constant Frequency Pattern Method

The overall control structure of the constant frequency pattern method is shown in Fig. 1 [5].

In Fig. 1, the position error information can be obtained by (1)

$$\hat{\theta}_{err} = \frac{-1}{\hat{\omega}_r \lambda_f} \tag{1}$$

where $\hat{\theta}_{err}$ is the position error from the d-axis current regulator output voltage, $\hat{\omega}_r$ indicates the estimated electrical rotor velocity, and λ_f is the flux linkage of the permanent magnet. The sensorless control block diagram is shown in Fig. 2.

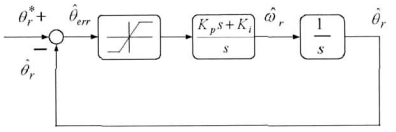

Fig. 2 Block diagram of sensorless control structure (Region II).

The position error can be controlled at zero by the rotor position tracking PI controller. From (1), in the zero and low speed region, the position error has a large value and therefore starting may fail from standstill. However, it is valid in the high speed region (Region II).

3. Analysis of Proposed Sensorless Control in Frequency domain

To overcome this problem, the position error in the zero and low speed region (Region I) should be limited as in (2).

$$\hat{\theta}'_{err} \approx \frac{V^e_{ds\_fb}}{\mathrm{sgn}(\hat{\omega}_r) k \cdot \lambda_f} \hat{\theta}_{err} = \frac{V^e_{ds\_fb}}{K \cdot \lambda_f} \hat{\theta}_{err} \quad , \tag{2}$$

where K has a constant value and then the sensorless block diagram can be redrawn as shown in Fig. 3.

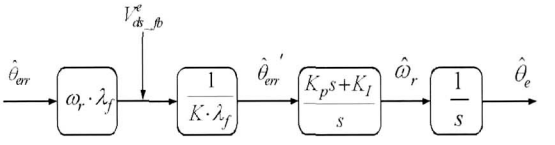

Fig. 3 Block diagram of sensorless control for zero and low speed operation (Region I)

From the basic definition of the phase margin, the following equation for phase margin ϕ_m is obtained [6].

$$\phi_m = \arg[G_c(j\omega_g) G_p(j\omega_g)] + \pi \quad , \tag{3}$$

where $G_c(s)$ and $G_p(s)$ in Region II are given by

$$G_c(s) = \frac{K_p s + K_i}{s} \tag{4}$$

$$G_p(s) = \frac{1}{s} \tag{5}$$

and the system bandwidth ω_g is

$$\left| G_c(j\omega_g) G_p(j\omega_g) \right| = 1 \ . \tag{6}$$

Substituting (4) and (5) into (3) and (6) gives

$$\omega_g = \sqrt{\frac{K_p^2 + \sqrt{K_p^4 + 4K_i^2}}{2}} \tag{7}$$

$$\phi_m = \arctan\frac{K_p}{K_i}\sqrt{\frac{K_p^2 + \sqrt{K_p^4 + 4K_i^2}}{2}} \tag{8}$$

4. Tuning Formulas for Rotor Position Tracking PI Controller

Using (7) and (8), solving for PI gains gives

$$K_p = \omega_g \sqrt{\frac{(\tan\phi_m)^2}{1+(\tan\phi_m)^2}} \tag{9}$$

$$K_i = \omega_g^2 \sqrt{\frac{1}{1+(\tan\phi_m)^2}} \tag{10}$$

Many engineers think directly in terms of ϕ_m in judging whether a control system is adequately designed. Practically, a desirable ϕ_m is often considered as

$$30^0 < \phi_m < 60^0 \tag{11}$$

Usually, the estimator poles can be chosen to be 2 or 6 times faster than the controller poles. This is to ensure a more rapid delay of the estimator error compared with the desired dynamics. Therefore, the bandwidth of the rotor position tracking PI controller becomes higher than that of the speed controller.

From Fig. 3, $G_c(s)$ in Region I is given by

$$G_c(s) = \frac{K_p^{'}s + K_i^{'}}{s}, \tag{12}$$

where $K_p^{'} = \frac{\hat{\omega}_r}{K}\cdot K_p$, $K_i^{'} = \frac{\hat{\omega}_r}{K}\cdot K_i$.

Hence, the bandwidth of the rotor position tracking PI controller in the zero and low speed region can be obtained as

$$\omega_g = \sqrt{\frac{(\frac{\omega_r(t)}{K}\cdot K_p)^2 + \sqrt{(\frac{\omega_r(t)}{K}\cdot K_p)^4 + 4\cdot(\frac{\omega_r(t)}{K}\cdot K_i)^2}}{2}} \tag{13}$$

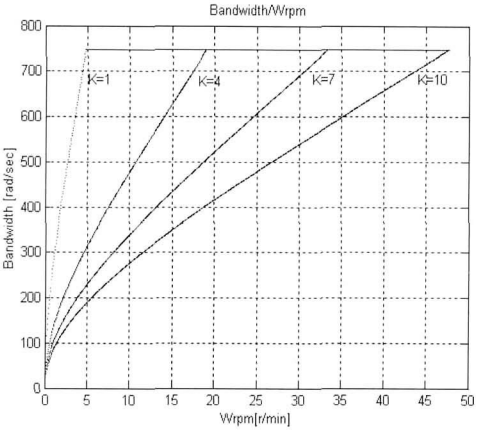

Fig. 4 Bandwidth locus of proposed PI controller according to estimated rotor velocity.

In (13), it can be seen that the bandwidth of the proposed position tracking PI controller is varying according to the estimated velocity as shown in Fig. 4. This means that the magnitude of the motor back emf voltage is proportional to the rotor speed and it is very small at the low speed region. Then, during zero speed, the rotor position and velocity have sluggish dynamics because the varying gains are extremely low in this region In Fig. 4, the bandwidth of the rotor position tracking PI controller is set to 750 rad/s. Decreasing K will raise the loop bandwidth to a lower speed region. For example, if K is 1, the sensorless loop gain will become 750 rad/s above 5 r/min. From this result, the designers can easily determine the possible operating range with a desired bandwidth.

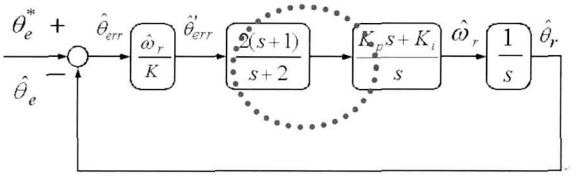

Fig. 5 Block diagram of sensorless control with lead compensator during low speed operation.

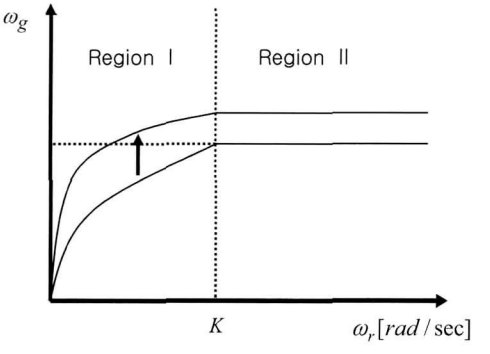

Fig. 6 Bandwidth locus of proposed PI controller with lead compensator.

To boost the bandwidth of this region, a lead compensator is introduced to recover the loop dynamics in the low speed region as shown in Fig. 5. This may improve the estimation dynamics of rotor speed in the low speed region.

5. Simulation Results

The proposed sensorless algorithm was tested on a 400W PMSM in Table I using Matlab/Simulink. The bandwidths of the speed controller and rotor position tracking PI controller were set to 150 rad/s and 750 rad/s, respectively. The phase margin was 50° with K set to 1. The sampling periods of the current and the speed control loop were 100 μs and 500 μs, respectively. The load inertia was coupled to the motor and the inertia ratio was 10:1.

Fig. 7 shows the estimated and actual speed with varying speed commands from zero to 500[r/min]. From the top, speed command, estimated speed, and actual speed for monitoring are depicted. The estimated speed properly follows the speed command in both the low and high speed ranges.

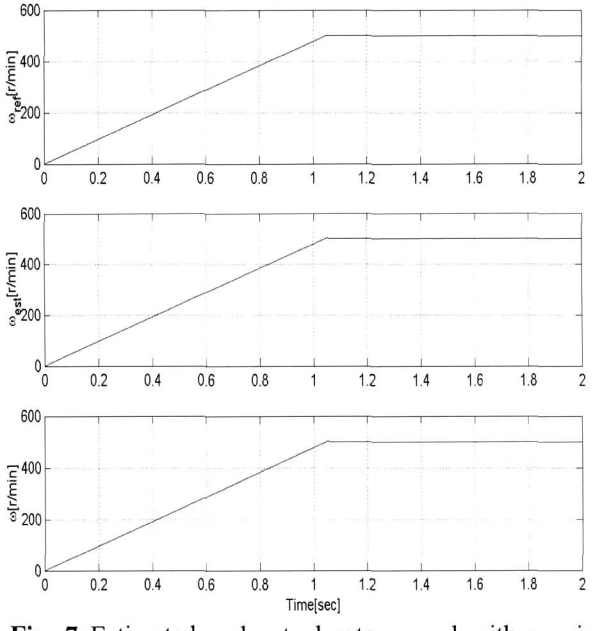

Fig. 7 Estimated and actual rotor speed with varying speed commands (0 to 500[r/min]).

Fig. 8 indicates the responses of the proposed sensorless scheme for the 500 r/min step speed command. In this test, the proposed algorithm does not lose its estimation capability.

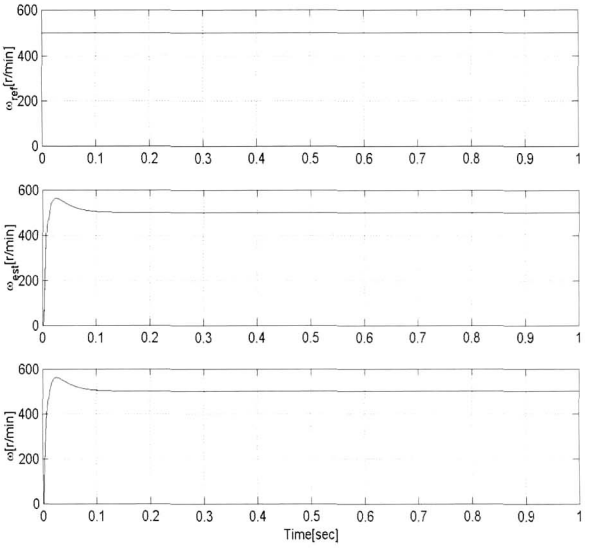

Fig. 8 Estimated and actual rotor speed with step speed command (0 to 500[r/min])

Table 1 Ratings and Known Parameters of PMSM under Test

3-phase, 220[V], 600 [W], 8 Poles	
Rated speed	3000 r/min
Torque constant	0.477 Nt-m/A
Moment of inertia	1.1×10^{-4} Kg-m^2
Back emf constant	0.352 Vrms/rpm

Fig. 9 shows the responses of the proposed sensorless scheme with 5 r/min speed command under 100% load torque condition. From the top, speed command, estimated speed, actual speed for monitoring, position error, and load torque are depicted. The rotor position estimation error is confined to nearly zero in transient state as well as in steady state.

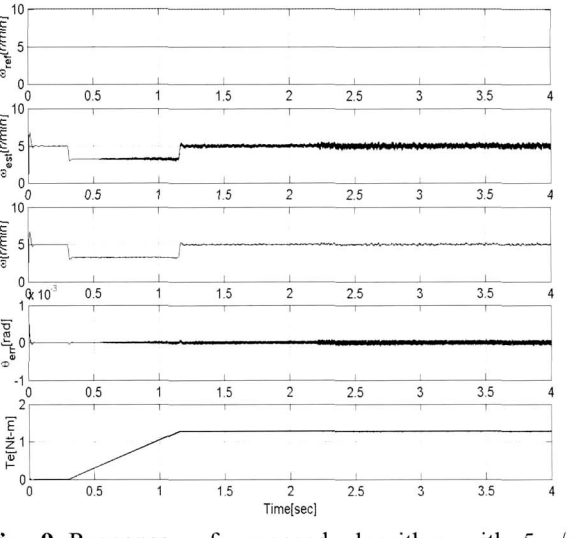

Fig. 9 Responses of proposed algorithm with 5 r/min speed command under 100% load condition.

6. Experimental Results

Intensive tests were performed to verify the presented study. The algorithm was programmed and installed to a commercial 600-W PMSM without rotor saliency, which is the same motor that has been used in the simulation tests. The PWM VSI inverter consisted of 20kHz switching IGBT modules and was controlled by the control board using a digital signal processor (DSP), TMS320VC33 120MHz. A 750-W DC motor was coupled with a 600-W PMSM in order to apply the load torque as shown in Fig. 10. The bandwidths of the speed controller and the rotor position tracking the PI controller were set to 100 rad/s and 300 rad/s, respectively. The phase margin was 50° with K set to 10, and control mode switching occurred at 25 r/min. The sampling periods of the current and the speed control loop were 50 μs and 1 ms, respectively.

Fig. 11 shows the estimated and actual speed/position with a step speed change from zero to 50 r/min. From the top, estimated speed, measured speed using 1024 p/r encoder for monitoring, estimated position, and measured position are depicted. The test motor has eight poles, so 50 r/min means that the rotor frequency is about 3.3 Hz. It can be seen that the estimated speed is in close agreement with the actual speed under transient state as well as steady state around zero frequency. From this test, it is worth mentioning that the proposed sensorless PI estimator provides satisfactory transient performance even at the speed of 3.3 Hz. This improvement is mainly due to the derivation of PI gain formulas based on the frequency domain analysis and the selection of desired bandwidth considering the effect of constant K.

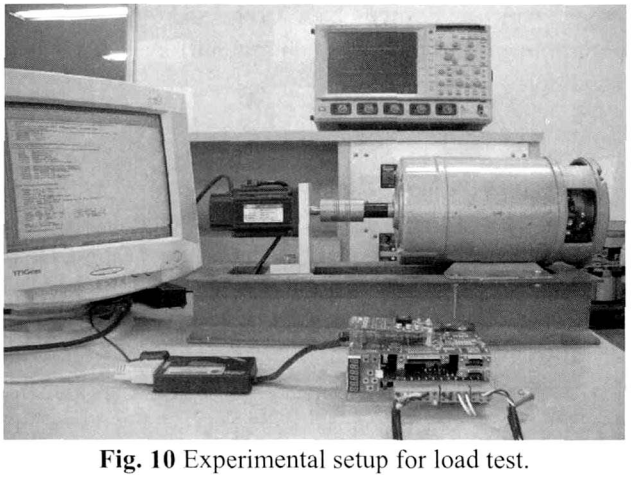

Fig. 10 Experimental setup for load test.

Fig. 12 presents the performance of the rotor position error in electrical degrees with 50 r/min speed command. The rotor position estimation error is confined to nearly zero in steady state.

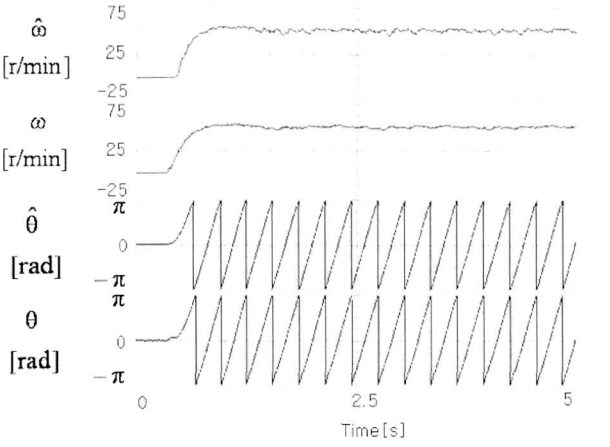

Fig. 11 Estimated and measured speed/position with a step 50 r/min command change.

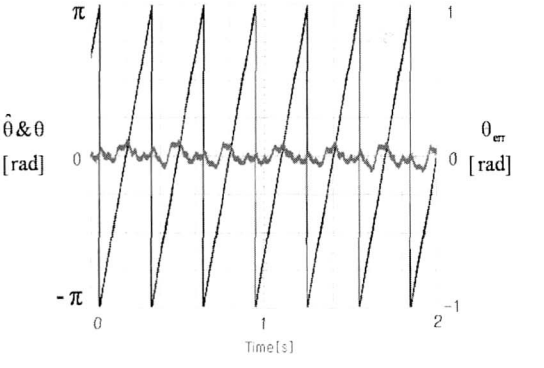

Fig. 12 Responses of position error with 50 r/min speed command.

In Fig. 13, the performance of the proposed method is again assessed by changing the speed command from 100 to 50 to 150 r/min. From the top, speed command, estimated speed, actual speed for monitoring, and q-axis current are depicted. At very low speeds, the proposed algorithm does not lose its estimation capability under speed transient change and the speed control is stable at transient and steady state.

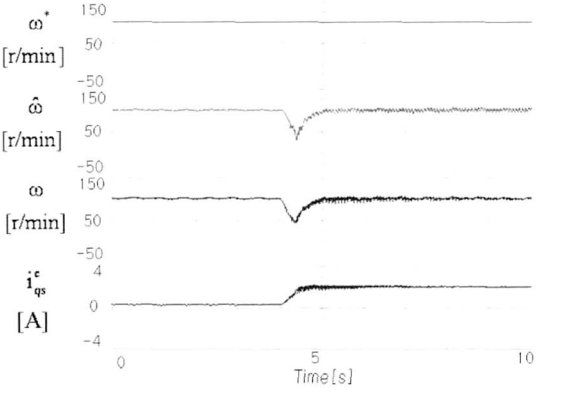

Fig. 14 Responses of proposed algorithm with 100 r/min speed command under half-rated load condition.

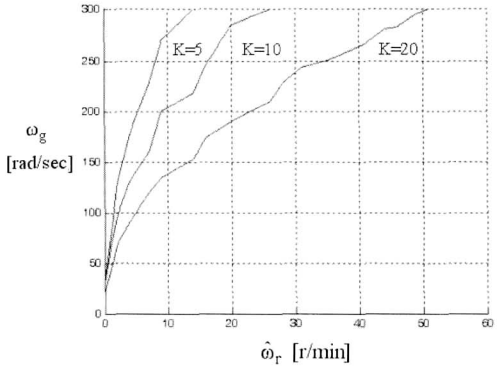

Fig. 15 Experimental bandwidth locus according to estimated rotor velocity.

Fig. 14 presents the response of the proposed sensorless scheme with 100 r/min speed command under half-rated load condition. This demonstrates that the speed estimation and control are robust during a transient load torque change.

Fig. 15 illustrates the experimental bandwidth trajectories of the rotor position tracking PI controller according to the estimated velocity. As expected, when K is 10, the sensorless loop gain becomes 300 rad/s around 30 r/min. From this result, it is concluded that the designers can decide the control authority at a given operating frequency before startup.

Fig. 16 indicates the speed transient responses under load variation from 0 to 1 p.u. when speed command is set to 100 r/min. From the top, speed command, estimated speed, q-axis current command, and q-axis current are depicted. Compared to the no load or half-rated load condition, the speed ripple is somewhat increased, which is mainly caused by the dead-time effects, current measurement errors, and mechanical coupling eccentricity. The proposed algorithm does not lose its estimation capability even under rated load condition. This result shows that the proposed sensorless algorithm yields a satisfactory low-speed control in the vicinity of zero frequency under rated load change.

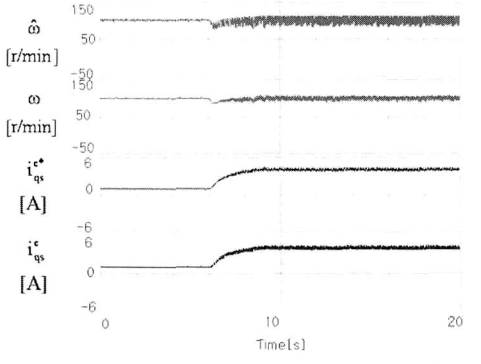

Fig. 16 Transient responses with 100 r/min speed command under rated load condition.

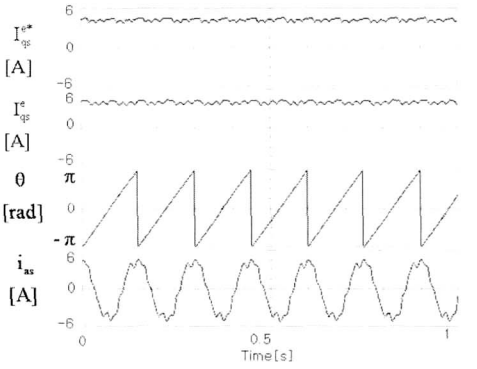

Fig. 17 Steady-state responses with 100 r/min speed command under rated load condition.

Fig. 17 is a plot of the steady state estimated rotor position and controlled currents under full load condition while the motor is running at constant speed 100 r/min. As can be seen from the heavy load tests, the control performance is very robust in the transient state as well as in the steady state.

7. Conclusion

This paper has described a new sensorless control technique for a non-salient PMSM. The proposed scheme is based on the d-axis current regulator output voltage of the drive system, which contains the rotor position error information. The rotor velocity can be estimated through a rotor position tracking PI controller that controls the position error at zero. For zero and low speed operation, the PI gain of the rotor position tracking controller has a variable structure according to the estimated rotor velocity. The designers can easily determine the possible operating range with a desired bandwidth and the proposed algorithm enables the speed control under even 100% load condition.

References

[1] R. Wu and G. R. Slemon, "A Permanent Magnet Drive without a Shaft Sensor", *IEEE Trans. on Ind. Applications*, vol. 27, No. 5, Sep./Oct., 1991, pp. 1005-1011.

[2] N. Ertugrul and P. Acarnley, "A New Algorithm for Sensorless Operation of Permanent Magnet Motors", *IEEE Trans. on Ind. Applications*, vol. 30, No. 1, Jan./Feb., 1994, pp. 126-133.

[3] J. S .Kim and S. K. Sul, "New Approach for High Performance PMSM Drives without Rotational Position Sensors", *IEEE Trans. on PE*, vol. 12, No. 5, 1997, pp. 904-911.

[4] J. H. Jang, S. K. Sul, J. I. Ha, K. Ide, and M. Sawamura, "Sensorless Drive of SMPM motor by High Frequency Signal Injection", IEEE APEC02 Conf. Rec., 2002, pp. 279–285.
[5] B. H. Bae, S. K. Sul, J. H. Kwon, and J. S. Shin, "Implementation of Sensorless Vector Control for Super-high Speed PMSM of Turbo-compressor", IEEE IAS01 Conf. Rec., 2001, pp. 1203–1209.
[6] W. K. Ho, C. C. Hang, and J. H. Zhou, "Performance and Gain and Phase Margins of Well-known PI Tuning Formulas", *IEEE Trans. on Cont. Syst. Technol.*, vol. 3, 1995, pp. 245-248.

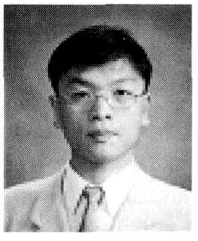

Jong-Kun Lee
He received the B.S. and M.S. degrees from Yeungnam University, Kyongbuk, Korea, in 2002, 2005, respectively.
He is with the Robot Institute, Daewoo Shipbuiding & Marine Engineering Company Ltd., Geoje City, Korea. His specific research interests are electrical machines, high-performance electrical machine drives a nd active power filters.

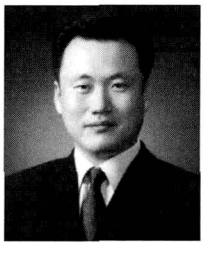

Jul-Ki Seok
He received the B.S., M.S., and Ph.D. degrees in electrical engineering from Seoul National University, Seoul, Korea, in 1992, 1994, and 1998, respectively. From 1998 to 2001, he was a senior engineer with the Production Engineering Center, Samsung Electronics, Suwon, Korea. Since 2001, he has been a member of the faculty of the School of Electrical Engineering and Computer Science, Yeungnam University, where he is presently an Assistant Professor. His specific research interests are in high-performance electrical machine drives, control and analysis of linear hybrid stepping motor, and nonlinear system identification as related to the power electronics field.